

Predictive Robotic Harvesting Based on Non-Stationary Markov Chain Vegetation Cycle Model and Crop Simulation

Andrzej M.J. Skulimowski

AGH University of Kraków and Progress & Business Foundation, Kraków, Poland

ams@agh.edu.pl

Abstract

This article presents methodological foundations for the predictive harvesting of berry fruits with autonomous robots. By predictive harvesting we refer to identifying the areas of the crop that guarantee the best yield. Additionally, harvesting in these areas may optimize other performance indicators. The reported research focuses on the construction and subsequent validation of a vegetation cycle model for strawberries in covered crops such as foil tunnels and greenhouses. The model is calibrated with real-life observations of selected strawberry variant growth, which depends on insolation, temperature, and humidity. The vegetation cycle model is embedded into a crop simulation that records all fruits picked by robots in the greenhouse. This application calculates the sites with the highest expected density of ripe fruit to initiate the next day's harvest. The multicriteria optimization procedure maximizes harvest yield and harvest efficiency, while minimizing the mass of non-harvested ripe fruits.

Keywords: Predictive harvesting, Autonomous agricultural robots, Strawberry vegetation cycle, Non-stationary Markov chains, Harvest optimization.

1. Introduction

This study aims to provide a formal foundation for the efficient predictive harvesting of berry fruits such as strawberries using autonomous robots. By *predictive harvesting* we are referring to a procedure for assigning the robots tasks in the areas of the crop that guarantee the highest yield. The optimization of other indicators of harvest efficiency can also be taken into account. Research presented in this article focuses on the construction and subsequent validation of a vegetation cycle model for strawberries in covered crops such as foil tunnels and greenhouses. In these environments, strawberries are planted in separate soil segments arranged along a so-called gutter, which is a linear structure, typically suspended within the structure of a greenhouse. As a result, all plants

bear fruit at a picking height of about 1.2 meters, conveniently for both humans and robots. The crop for which the model presented here has been built consists of 8 double-sided gutters, each approximately 95m long and divided into 0.6 m long segments. The spaces between gutters range from 1.2 to 1.5m in width providing sufficient room for a platoon of robots moving in a designated direction. The above configuration represents a standard strawberry crop unit within a plantation currently spanning 80'000 m².

We assume that the strawberry fruits are harvested by autonomous mobile robots equipped with a gripper that features a cutting mechanism. A high-resolution camera on a robot mast comes with software capable of recognizing the development stage of all fruits in a segment during a single scan. Furthermore, the robots can communicate with each other and with a supervisory control panel via a WiFi 6-based Internet of Vehicles (IoV) standard which provides access to the knowledge base of the crop, the configuration of the working environment, as well as the model of the vegetation cycle of the plants along with its current outcomes. This information is used to determine a harvesting strategy by selecting an optimal sequence of gutter sections and assigning them to the robots. Each section may contain one or more adjacent segments on the same side of a gutter. The robot team coordinator assigns sections to individual units based on anticipated total yield, harvesting efficiency and quality, using the estimated number of ripe strawberries in particular gutter segments and parameters of the path from the robot's current location to the section under question. Thus, section assignment is an instance of a combined multicriteria multiple robot path planning - multiple robot task allocation problem (MRPP-MRTA, cf. e.g. Korsah et al., 2013).

In the anticipatory coordination model (Skulimowski, 2016; Skulimowski & Karimi, 2023) used here, the coordinator is the robot with the most comprehensive knowledge of states and positions of other robots, as well as the condition of the crop. Before updating optimization and coordination calculations, this robot gathers from fruit picking

robots all available information about the fruits that have been harvested or scanned but left on gutters. During this activity the coordinator uses its computing power exclusively for coordination purposes, afterwards it can resume picking strawberries.

The model presented in this article can be used either to simulate off-line strawberry cultivation and harvesting, or it can be installed on robots as a component of coordination software in a greenhouse environment. It can also be integrated with Agricultural Internet of Things (AIoT) software in the greenhouse, such as CloudVision (cf. www.sercom.eu).

1.1. Problem statement and its solution

Unlike human workers, fruit picking robots do not yet possess the full cognitive capability to identify the distribution of ripe fruits in the greenhouse. Due to the fruits hanging down on stalks and being obscured by leaves above, the vast majority of fruits cannot be assessed by stationary monitoring cameras. On the other hand, scanning a gutter segment with a hi-resolution fruit recognition camera is a time consuming process that takes up to 60 seconds per segment, regardless of whether the gutter is full of ripe fruits or empty. Thus arises the following problem:

Problem 1. Calculate the ripe fruit distribution in the greenhouse at a future time $t+\tau$, based on the record of previous harvests, information obtained from the vision systems of all fruit picking robots and greenhouse cameras, and a vegetation cycle model fed with past and forecasted meteorological data. ■

Problem 1 forms the basis for assigning gutter sections and paths to robots (MRPP-MRTA) which is the subject of another study. The current article focuses on building a strawberry vegetation cycle model that plays a pivotal role in crop forecasting, as no adequate existing model was found. Thus, the main specific subproblem of Problem 1, as applied to real-life implementation can be formulated as follows:

Problem 2. Given the initial distribution of seedlings of a certain strawberry cultivar in the greenhouse at time t_0 and information on the fruit growth process $\varphi(t,s,T)$, where s is the insolation and T is the accumulated heat derived from the internal greenhouse temperature curve, calculate the distribution of plants at each vegetation stage at time t . ■

Note that the term *vegetation stage* refers to fruit states defined in terms of robot cameras' capability to distinguish different stages of fruit growth. Furthermore, in Problem 2 humidity is omitted as a growth factor as it is assumed to be optimally controlled by existing greenhouse automation software.

As the fruit growth model in the solution to Problem 2 a non-stationary discrete Markov process is applied, with states corresponding to the successive developmental stages of the strawberry fruit. The *non-stationarity* of the process is reflected in transition probabilities that depend on the time spent in the current state. Strawberry harvesting is modelled as a control, which transforms the above model into a controlled Markov process with disturbances, such as the accidental harvesting of unripe or overripe fruit, overlooked ripe fruits on the gutter, as well as accidental damage or destruction by pests. Figure 1 below illustrates the application scheme of the model.

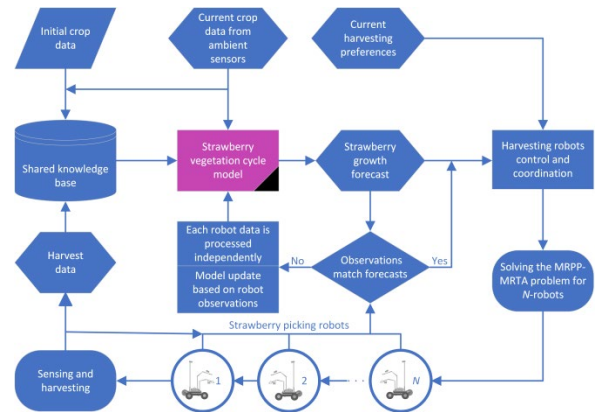


Figure 1. Embedding the strawberry vegetation cycle model into the robotic predictive harvesting.

1.2. The structure of this article

Section 2 presents an overview of strawberry vegetation modelling in the context of smart agriculture. In Section 3 we construct an 8-state model representing the successive developmental phases in the strawberry vegetation cycle, along with an additional state assigned to damaged or disease-affected fruits that are not harvested. The implementation of the model, its embedding into the simulation and control software, as well as computational experiments, are presented in Section 4. The experiments using a model calibrated with seasonal parameters gathered in 2023 demonstrated the adequacy of the modelling methodology used. The discussion in Section 5 reviews approaches to combining the model with a machine learning (ML) module and specifies how the observations of gutter segments and the identification of the actual distribution of fruit development can determine adjustments to model parameters in case of deviations from predictions. In the conclusion, we outline plans for further research, including the development of the growth model using fuzzy Markov chains, as well as an alternative fruit development description based on continuous Markov processes.

2. The parameters of the strawberry vegetation cycle and related research

As a so-called *non-climacteric* fruit, the strawberry cannot ripen after harvesting (cf. e.g. Abd-Elrahman et al., 2021; Fan et al., 2022). This means that only the ripe fruits can be harvested, in contrast to climacteric berries such as tomatoes or other fruits such as bananas. Additionally, the ripeness period of strawberry fruit is relatively short, and unpicked ripe strawberries spoil easily, which quickly renders them unsuitable even for industrial purposes. Ripe strawberries remaining on the gutter for a longer period of time, though still edible, may no longer be suitable for robotic harvesting and wholesale distribution due to their reduced resistance to crushing during harvesting and transportation. For this reason, the robotic strawberry harvesting is a demanding process that requires the anticipatory identification of ripe strawberries in the greenhouse and efficient harvesting, as soon as possible after they reach maturity. Moreover, robots must be equipped with robust sensors and grippers.

2.1. Physical characteristics of strawberries

The physical characteristics of ripe strawberries that impact harvesting decisions are the intensity of their color (specifically, it is the intensity of their redness), as well as the weight range and size of the strawberry. Additionally, individual strawberry varieties are characterized by:

- Varying ripening timelines, including differing durations spent in each of the states specified in Tables 1 and 2 in Section 3.
- The crush resistance of ripe strawberries.

The length of time a strawberry remains in a given stage of the vegetation cycle (modelled as a Markov process state) affects the probabilities of moving to the next state or remaining in the current state. These values form a matrix of state transition probabilities (see Section 3). Both the physical properties and the parameters that define the states of the strawberry from the perspective of making harvesting decisions are specific to each variety. Here, we focus on varieties suitable for gutter cultivation in foil tunnels.

In order to build a strawberry vegetation cycle model, we need to determine:

- The physical characteristics of the different stages of strawberry development for each variety grown.
- The temporal characteristics of the strawberry vegetation cycle from the perspective of schedu-

ling automatic recognition of ripe fruit and assigning tasks during robotic harvesting.

In the strawberry fruit growth model adopted for robotic harvesting, the physical properties of the fruit recorded by the robot's cameras and analyzed before making the harvest decision are:

- Color (measured with RGB or CIELAB standards),
- Dimensions (maximum linear size or 3D outline in mm).

Further physical characteristics of the strawberry that are relevant to the robot's harvesting decision but difficult to measure using 2D images alone include:

- Weight (in g),
- Regularity of fruit shape,
- Crush resistance of the ripe strawberry (the maximum pressure in N/cm^2 that does not crush the fruit).

Color and dimensions are determined from 2D camera imagery, while mass and shape are derived from a 3D scan. Crush resistance is measured using a force sensing resistor or another strain gauge sensor integrated into the gripper.

Additional physicochemical characteristics that can be studied through hyperspectral (Gao et al., 2020) or near-infrared imaging methods (NIR, cf. Wendel, Underwood, & Walsh, 2018) are:

- Presence of chemical compounds indicative of fruit ripeness (Sim et al., 2020).
- Presence of lesions caused by plant diseases.

Although measuring physicochemical characteristics can significantly increase the accuracy of strawberry ripeness verification (Ge et al., 2020), this is not adopted in the current concept of the robot sensor system due to a cost increase of commercial robot deployment. In addition, the use of more affordable spectroradiometric or colorimetric techniques to measure color intensities may have a similar effect.

The primary quality characteristics of strawberry fruit is its ripeness, defined by a set of parameters that determine its suitability for harvesting and consumption. In large-scale production, certain commercial standards apply, which are crucial for the automatic recognition of ripe strawberries. For the vision system that automatically classifies fruits, installed on the robotic platform, the key measurable characteristic determining the ripeness of the fruit is its color. However, the other characteristics mentioned above may also be taken into account.

Additional characteristics of strawberry fruit, which are partly qualitative and partly quantitative in

nature, include the expected shelf life, flavor profile (juice and monosaccharide content), and uniformity of harvested fruit size. With the exception of size uniformity, these parameters are not measured during robotic harvesting.

2.2. The strawberry vegetation cycle research to date

The vegetation cycle model presented in this report is designed for strawberry varieties such as *Hademar* and *Furore* grown in large industrial plantations in Central Europe. In developing the model, several studies employing diverse approaches to modelling strawberry growth were considered, such as logistic models of accumulated heat (Diel et al., 2022), YOLO (An et al., 2022). The latter study used five stages of strawberry fruit growth. Some researchers have based strawberry growth parameters not only on average air temperature and sunlight, as assumed in our model, but also on soil temperature, relative humidity in the foil tunnel, soil moisture, soil electrical conductivity, CO₂ concentration, photosynthetic radiation activity and water vapor pressure deficit (Sim et al., 2020).

Clausse et al. (2007) used a Markov chain model of apple tree fruit growth. While this model is not transferable to the vegetation cycle of berries due to differing assumptions, it confirms the general methodology of modelling fruit growth as a Markov process which is adopted in this article. Similarly, Orchard et al. (2019) used a hidden state Markov model to describe post-harvest and sales logistics of blueberries. Lee et al. (2020) applied the combined effects of weather conditions to forecast soft fruit yields. The influence of temperature and moisture on strawberry ripening has also been studied by Sønstebj et al., (2016), Tang et al. (2020), Twitchen et al. (2021), Abd-Elrahman et al. (2021).

In recent years, there has been a growing number of publications reporting research on and verification of fruit growth parameters using hyperspectral imaging (cf., for example, Wendel et al., 2018). This line of research is also recommended for the further development in robotic strawberry cultivation, particularly for detecting of infected, parasite-affected, overripe or rotten fruits. To handle the large amount of hyperspectral data in real time, deep learning techniques will become indispensable (Ridho & Irwan, 2021). To prevent the spread of diseases and parasites, the removal of such fruits should be handled by dedicated robots equipped with specialized grippers that include disinfection capabilities and differ from those used for ripe fruit harvesting.

3. Strawberry vegetation cycle as a non-stationary controlled Markov chain

3.1. Development stages of strawberry fruits

In order to build a model for robotic harvesting in covered crops for each strawberry variety, the ranges of physical properties of the harvestable fruit should be determined, along with a similar characterization of the other stages of the vegetation cycle. It is also essential to determine how the time spent in each state depends on sunlight, temperature, air humidification and humidity in the crop environment. For the purposes of automatic recognition and robotic autonomous harvesting, the following characteristics of strawberries, estimated from observations of the physical characteristics described above, are crucial:

- **Age of the fruit expressed in days**, where: $t = 0$ correspond to a freshly sown strawberry, $t = t_1$ represents the first day after germination of the strawberry (which is the first day when the plant can be detected by the robot's vision system), ..., and $t = n$ represents the strawberry's age n days after sowing,
- **State** is a stage in the development (vegetation cycle) of a strawberry. We can identify 9 states $S_0, S_1, S_2, \dots, S_8$, where S_0 is a freshly planted (non-detectable) strawberry, S_1 to S_6 are subsequent developmental stages, S_7 and S_8 represent strawberries unfit for harvesting (S_7 – overripe, S_8 – rotten, damaged, or affected by pests, etc.), cf. Table 1.

State S_0 – freshly planted strawberry – is unobservable by the robots, i.e. it lacks visible vegetative features. Information about the distribution of planted strawberries is provided by the crop manager, along with the number of days since sowing. Due to the different sowing dates of each gutter, this value may not always be available. The strawberries' germination rate depends on the seed quality, physical characteristics of the soil, environmental factors, and this dependence is specific to individual varieties of the plant.

As noted above, for each state, the weight, size, and color of a strawberry can be described as intervals with boundaries corresponding to the probability that the $1-2 \cdot p_0\%$ characteristics of all fruits in a given state fall within are the associated interval. It can be assumed that parameter deviations are symmetrical, meaning that the same percentage of fruits has parameters below the lower bound of the interval as above the upper bound. Based on the data from the plantation, the value $p_0 := 2\%$ was used. Example values for "size" r (the largest dimension of the strawberry

of a given variety) and weight m are given in Table 2. Descriptions of the states characterizing the strawberry vegetation cycle are presented in Table 1.

There are multiple ways to classify the different stages of the fruit vegetation cycle. The description method depends on the actual morphological differences of the different varieties, the technical ability to recognize these stages (including model parameter identification using ML methods), as well as the harvesting needs based on the harvesting technique and intended use of the fruit. For example, the definition of a harvestable strawberry for industrial purposes will differ from that of a dessert strawberry intended for direct consumption. For strawberries in covered crops, we have assumed the following series of states to characterize their vegetation cycle:

Table 1. Parameters of strawberry states in greenhouse crops, Hademar and Furore varieties.

State	Descriptions of plant/fruit states	Period of remaining in state S_i	Time of remaining in state S_i in days		
			Min	Avg	Max
S_0	Plants freshly planted, no external parts	$[0 < t \leq T_1]$	0	10	15
S_1	Plants are visible, but no fruit for identification yet	$[T_1 < t \leq T_2]$	15	23	29
S_2	Very small green fruits, size $r < 10$ mm (size and weight according to Table 2)	$[T_2 < t \leq T_3]$	32	35	38
S_3	Small green fruits, size $r < 25$ mm	$[T_3 < t \leq T_4]$	49	51	53
S_4	Small fruits, size $r < 30$ mm, noticeable color change (green color turns to yellow)	$[T_4 < t \leq T_5]$	51	53	55
S_5	Fruits almost ripe, red color does not cover the entire fruit surface	$[T_5 < t \leq T_6]$	53	55	57
S_6	Ripe fruits, ready for harvesting	$[T_6 < t \leq T_7]$	55	57	59
S_7	Overripe, spoilt fruits	$T_7 < t \leq T_8$	57	59	62
S_8	Fruits attacked by vermin, pests, or microorganisms, or damaged during ripening	any $t > T_1$	NA	NA	NA

Data in the above table is based on observations collected during vegetation cycles in the years 2022 and 2023, provided for research purposes by the crop owner. The initial growth model was calibrated using this data and will be further refined to obtain a better fit to the observations. The parameter t in Table 1 refers to the time since sowing, and the values T_1 to T_7 represent the characteristic parameters of the vegetation cycle for a given strawberry variety. These parameters depend on the accumulated insolation, absorbed thermal energy from environment, air humidity and moisture level of the gutter substrate.



Figure 2. States of strawberries to be ready to harvest (own composition of open web images).

An example of strawberry fruit development stages is shown in Figure 2. The physical properties correspond to the states of the fruit development cycle, as defined in the following table.

Table 2. Physical parameters of strawberries in greenhouse crops, samples (cf. Figure 4)

State	Fruit/plant description	Size r (linear in mm)			Fruit weight m (in g)		
		Min	Avg	Max	Min	Avg	Max
S_2	Very small green fruits	$x_{2min} = 5$	$x_2 = 7$	$x_{2max} = 10$	$w_{2min} (NA)$	$w_2 (NA)$	$w_{2max} (NA)$
S_3	Small green	15	20	25
S_4	Unripe fruits	20	25	30	-	-	-
S_5	Almost ripe	22	35	55	15	25	50
S_6	Ripe fruits	22-25	35	55	15	25	50
S_7	Over-ripe fruits	x_{7min}	x_7	x_{7max}	w_{7min}	w_7	w_{7max}

As assumed earlier, the terms "minimum" and "maximum" in the tables above refer to the probability that at most $p_0=2\%$ of fruits are smaller or lighter than the minimum size/weight, and at most 2% of fruits are larger or heavier than the maximum size/weight. During the vegetation season, as observational data is collected during harvesting, it is also possible to estimate the standard deviation and quantiles for all parameters.

All states are ordered according to the progression of the vegetation cycle with the exception for state S_8 (disease-affected fruit, unfit for harvest), which the strawberry can transition to at any time. The distinction between non-harvestable fruit in states S_7 and S_8 is critical for assessing the risks to the entire crop from disease changes caused by microorganisms (bacteria, fungi, viruses). In the state S_7 (overripe, but not disease-affected), it is assumed that these threats are not yet present, so overripe strawberries classified in this state should be removed from the gutters. A separate robot could be assigned for this task, or alternatively overripe and damaged strawberries could be removed manually. Due to the potential for disease transmission, disease-affected strawberries should not be picked with the same gripper as those intended for consumption.

3.2. Strawberry vegetation cycle model

In this section we describe the strawberry vegetation cycle as a non-stationary Markov chain with a matrix of transition probabilities between the

states listed in the previous section. In considering general models, we assume that there are N states, allowing for the analysis of models with a reduced number of states. However, all simulation calculations presented in Section 4 were conducted for $N=8$. These probabilities depend on the duration in the current state, making it a non-stationary process.

The probabilities of changing the state of a strawberry variety v fruit at time t , are represented as the following matrix:

$$P_v(t, [\tau, s, h, T, \dots]) := \begin{bmatrix} p_{11} & p_{12} & 0 & 0 & 0 & 0 & 0 & p_{18} \\ 0 & p_{22} & p_{23} & 0 & 0 & 0 & 0 & p_{28} \\ 0 & 0 & p_{33} & p_{34} & 0 & 0 & 0 & p_{38} \\ 0 & 0 & 0 & p_{44} & p_{45} & 0 & 0 & p_{48} \\ 0 & 0 & 0 & 0 & p_{55} & p_{56} & 0 & p_{58} \\ 0 & 0 & 0 & 0 & 0 & p_{66} & p_{67} & p_{68} \\ 0 & 0 & 0 & 0 & 0 & 0 & p_{77} & p_{78} \\ 0 & 0 & 0 & 0 & 0 & 0 & 0 & 1 \end{bmatrix} \quad (1)$$

where p_{ij} are the transition probabilities of the fruit from state S_i to state S_j in a unit of time (in this model, one day), defined for day t of the cycle and dependent on all variables included in the definition of P_v . In particular, for $2 \leq j < N$ ($N=8$) all transition probabilities p_{ij} are non-decreasing functions of time τ_i that the fruit has remained in the i -th state. By assumption, the p_{iN} probabilities are constant while the fruit has remained in the i -th state. We do not consider the state S_0 after the strawberry is planted but before it germinates, as the plant is invisible to the robot's sensors during this time.

In the definition of the P_v probability matrix, we have included additional factors affecting the probabilities of interstate transitions, such as the time τ_i spent in the i -th state, cumulative insolation s , temperature T inside the greenhouse or foil tunnel while remaining in state S_i , and relative air humidity h . These factors will be discussed in more detail in the next section.

According to the model given above, the strawberry fruit can:

1. **Remain in a given state** (as determined by p_{ii} probabilities, $i=0,1,\dots,8$)
2. **Transition to the next state** (with an index exactly one greater than the current state), e.g., $p_{67}(t)$ is the probability of a strawberry transitioning from state S_6 to state S_7 in the time interval $[t, t+1]$.
3. **Become non-harvestable** (e.g., rot), transitioning to state S_8 from any other state in the time interval t to $t+1$. The probabilities of these events are described by the last column of P_v , e.g. p_{58} is the probability that a strawberry will rot while in state S_5 .

All other transitions are not allowed, meaning that it is not possible to skip a certain stage of development or return to an earlier stage. We also assume once a strawberry reaches state S_8 , it cannot return to a harvestable state ("curing the fruit"). All probabilities p_{ij} except p_{88} , which is always equal to 1, depend on the factors indicated in the definition (1) of P_v , including the time spent in state S_i .

Each variety of strawberry is characterized by a different transition matrix (1). For simplicity of calculation, we assume that for a given time t , a strawberry fruit is in only one state on the interval $[t, t+1)$. If it changes the state the new state $S(t+1)$ is admitted at the beginning of the next day. This means that the strawberry can change state only once per day. Under these assumptions, the evolution of states of a single fruit f is described by the equation

$$P(S(t+1)(f)=S_i) = \sum_{j=1}^N [\tilde{p}_{ij} P(S(t)(f)=S_j) - \eta_j(t)] - u_i(t) \quad (2)$$

where t is the current time and $S(t)$ is the current state of the fruit on day t , \tilde{p}_{ij} represents the cumulative probability of the fruit transitioning from state i to state j on day t , $u_i(t)$ is the i -th coordinate of the control vector $U(t)$ specifying the percentage of fruit harvested in state S_i on day t . In practice, harvesting refers only to fruit that is ripe (state S_6) or almost ripe (state S_5), and exceptionally overripe (state S_7). The value $u_8(t)$ describes the proportion of non-harvestable fruit, such as spoiled fruit removed from the growing area on day t . The remaining coordinates of $U(t)$ are equal to 0. In contrast, the coordinates of vector η_j describe the share of accidental abnormal harvesting or other types of loss, such as the total consumption by pests of fruit from the other states. The other notations follow those in equation (1).

Let $s(t, k, l)$ denotes a vector whose coordinates are the percentages of fruit in each state in the k -th segment of the l -th gutter. Denoting the total weight of fruit in this segment as $m(t, k, l)$, equation (1) and model (2) describing the evolution of a single strawberry generate the following iterative model with the variable $m(S(t))$ denoting the expected values of fruit weight in a given k -th segment of a l -th gutter in each state S_i on day t :

$$m(S(t+1)(f)=S_i) = \sum_{j=1}^N [\tilde{p}_{ij} P(S(t)(f)=S_j) - \eta_j(t)] - u_i(t), \quad (3)$$

where $1 \leq i \leq N$, $m = (m_1, \dots, m_N)$, $N=8$.

4. Implementation of the model

The implementation of the model presented in this section was carried out in the Matlab computing environment, version 2023b.

4.1. Crop model editor and vegetation cycle simulation

Below we present the editor of the working environment of autonomous robots for strawberry picking. This editor includes an interface to the strawberry vegetation cycle model, allowing users to define the initial state of the crop ("sowing") or randomly generate seed distribution for simulation purposes. The screen shots shown below simulate the real-life structure of the strawberry plantation where the experiments were performed. The gutters with fruit are divided into segments of 0.6m in length. These segments are also the smallest element of the vegetation cycle model, i.e. the properties of the fruit in each segment are averaged and their breakdown visualized. For clarity, the visualization focuses on the presence of ripe fruits. Segment colors reflect the presence of fruits in the most advanced state and depend on their absolute number and share. The full forecasted fruit structure in a segment can be viewed in a separate window that opens when clicking on the segment.

The above assumptions reflect the specificity of smart horticulture, where fruits in each segment grow from the same container with substrate and seeds acquired from a third-party commercial supplier. Furthermore, the range of a single scan of strawberries in the gutter covers at least the length of one segment (0.8m in the prototype picking robot). Figure 3 below shows the dashboard of the robot working environment simulation, while Figure 4 presents the first stage of building the strawberry vegetation cycle model when the initial duration of development stages and the corresponding dimensions of fruits are defined.

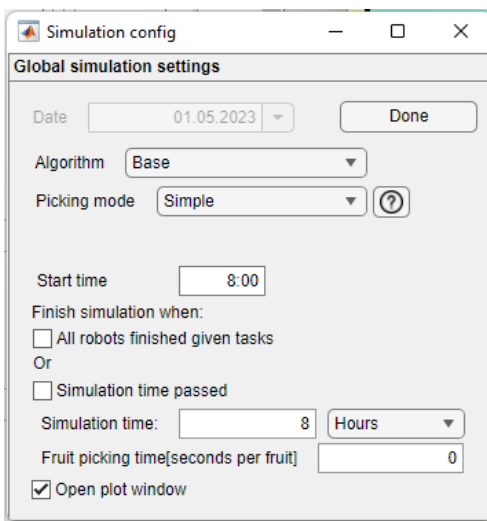


Figure 3. Harvest simulation editing dashboard with a choice of predictive harvesting algorithm.

Phase No.	Phase duration	Admissible duration	Average time from sowing	Average weight	Standard deviation	Average fruit diameter	Name	Description	Growth parameters	Add	Remove
1	10	5	10	0	0	0	seed	desc	EDIT	+	-
2	8	6	23	1	1	1	sprout	desc	EDIT	+	-
3	12	3	35	5	1	7	sprig	desc	EDIT	+	-
4	16	2	51	8	2	20	small unripe	desc	EDIT	+	-
5	2	1	53	50	15	25	unripe	desc	EDIT	+	-
6	2	1	55	50	15	35	almost-ripe	desc	EDIT	+	-
7	2	1	57	50	15	35	ripe	desc	EDIT	+	-
8	2	3	59	50	15	35	overripe	desc	EDIT	+	-
9	-	-	-	50	15	35	rotten	desc	EDIT	+	-

Figure 4. Fruit characteristics editing dashboard.

Figure 5 shows the working environment editing when the dimensions of the gutter crop and their arrangement in the greenhouse are defined.

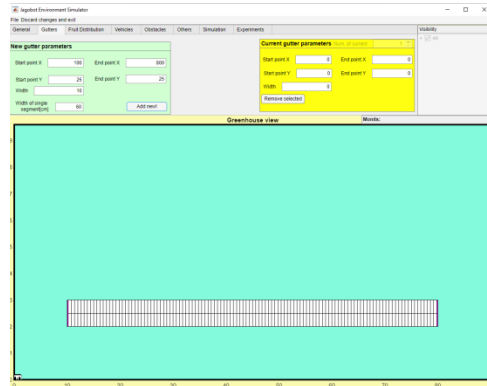


Figure 5. Working environment dashboard – editing an empty gutter before planting strawberries. Each rectangle denotes a single segment.

The following screenshots show the subsequent stages of modelling the strawberry vegetation cycle on eight previously defined gutters in the greenhouse. Green denotes unripe fruits, white fields indicate unown segments, blue indicates rotten fruits.

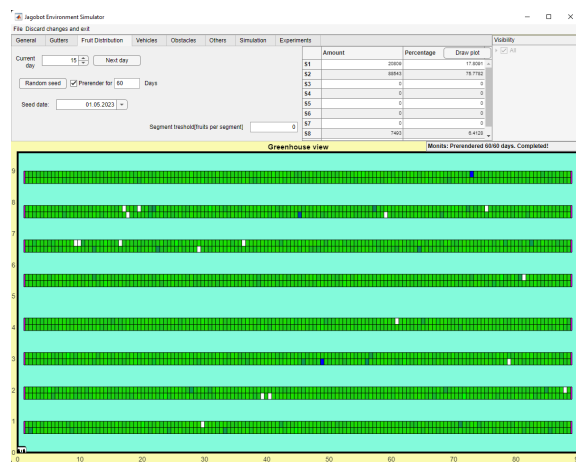


Figure 6. Visualization of the current state of strawberry growth 15 days after sowing. Numerical information about the strawberries in each state are provided in the top-right window.

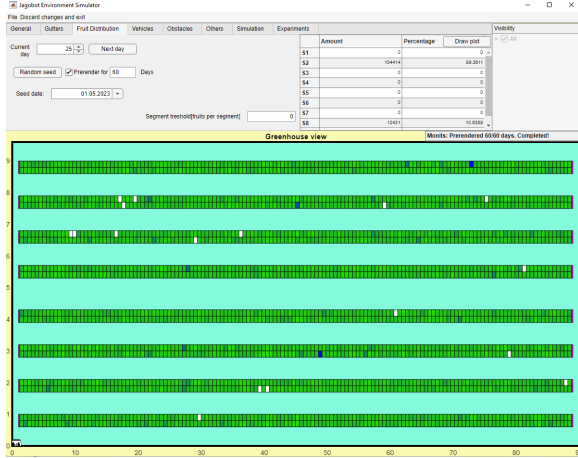


Figure 7. Visualization of the current state of strawberry growth 25 days after sowing. Dark green fields indicate strawberries in state S_4 .

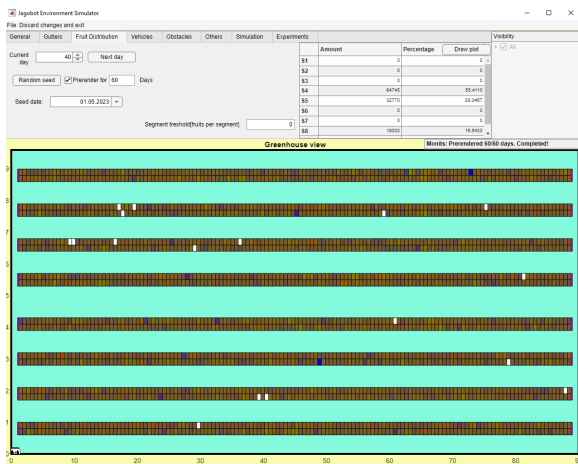


Figure 8. Visualization of the current state of strawberry growth 40 days after sowing. Reddish fields denote strawberries in state S_5 .

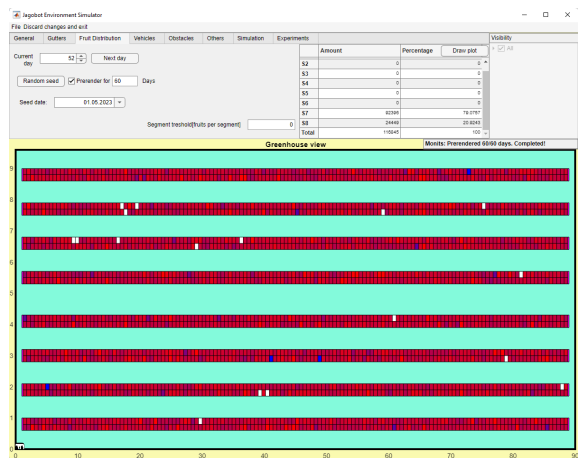


Figure 9. Strawberries after 52 days from sowing, with almost all of them in state S_6 (ripe)

The segments with ripe fruits (state S_6) in Figure 9 are marked in red, while the over-ripe strawberries (state s_7) are marked in dark red.

4.2. Embedding the vegetation cycle model in the simulation of strawberry harvesting

The harvest can be visualized in two modes: a full depiction of the state of the fruit's state (vector $s(i,k)$) in each segment of the gutter, or a simplified mode, where only ripe strawberries are depicted for better readability during the simulation run.

During harvesting, certain parametric rules govern the correctness and optimality of picking based on the structure of the vector $s(i,k,t)$ and the configuration of the strawberry harvesting robot, particularly its vision system. These rules are as follows. First, we assume that the fruit structure in the k -th segment of the i -th gutter is described at time t by the vector

$$s(i,k,t)=[S(i,k,t,1),\dots,S(i,k,t,8)]^T, \quad (4)$$

where $s(i,k,t,j)$ is the number of strawberries in state j , $j=1,2,\dots,8$, and $s(i,k,t,7)$ is the number of ripe, harvestable strawberries. We will denote the sum of the coordinates of the vector $s(i,k,t)$ by $ls(i,k,t)$.

The probability of picking a ripe strawberry is given by:

$$p_l(s,t)=1-a(1)*s(i,k,t,1)/ls(i,k,t)-\dots-a(6)*s(i,k,t,6)/ls(i,k,t)-a(8)*s(i,k,t,8)/ls(i,k,t)=1-\frac{\sum_{1\leq j\leq 8} a(j)s(i,k,t,j)}{ls(i,k,t)} \quad (5)$$

where $a(j)\leq 1$, $j=1,2,\dots,8$, are constants that depend on the robot's vision system's ability to recognize ripe strawberries, with $a(7)=0$. In particular, the coefficient $a(j)$ describes how the number of strawberry fruits in state j influences the recognition accuracy of ripe fruits in state S_7 , based on the principle that with the same number of fruits in a given class, smaller fruits are less influenced by omission, e.g., by occluding harvest-ready fruits for (in state S_6).

We assume that for $i=2,3,4,5,6$, the coefficients $a(i)$ are inversely proportional to the area of the fruit projection analyzed by the 2D camera, for example $a(i)=a_0/(7-i)^2$ with a_0 initially set to 1. During real-world fruit harvesting, the coefficients $a(i)$ are matched to the observations and updated by unsupervised ML or transfer learning methods.

In the recommended fruit picking robot configuration, the robot is equipped with two arms, one of which has an additional camera. In this case the coefficients $a(j)$ can be replaced by $a_2(j)=r_l a(j)$, e.g., with $r_l=0.5$, which corresponds to greater precision in recognizing ripe fruit and better quality harvesting. Similarly, the probability of being left

with a ripe strawberry in the k -th segment during harvesting amounts to:

$$p_2(t) := r_2 + [\sum_{1 \leq j \leq 8} b(j) s(i, k, t, j)] / s(i, k, t, 7), \quad (6)$$

where r_2 is the constant probability of leaving a ripe strawberry on the bush due to occlusion by leaves. If the robot is equipped with two arms, one of which has an additional camera, then we can assume that, for example, $r_2' = 0.1r_2$ and $b_2(j) = r_3 b(j)$, with $r_3 = 0.3$.

Figure 10 below shows the visualization of successive harvest stages and the resulting strawberry harvest rates in the coordination and control application which is linked to the vegetation cycle model. The main harvest indicators are presented in Figure 11.

The results indicate about a 30% increase in harvest performance when using the predictive harvesting approach, compared to the conventional harvesting algorithm that scans and picks fruits in each subsequent segment in the same gutter completing fruit picking one gutter before moving to the next. This efficiency increase is due to avoiding time-consuming scanning of segments with few ripe fruits.

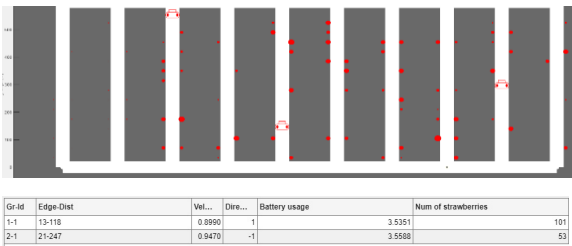


Figure 10. Harvest indicators window in the harvesting simulation application with an alternative way of visualizing the crop. Three fruit picking robots are marked in red.

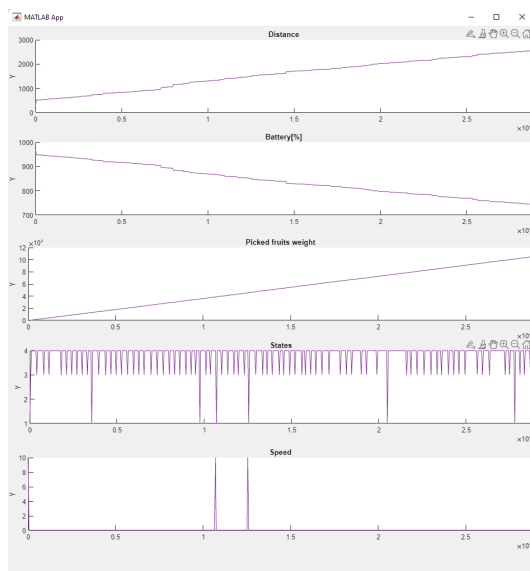


Figure 11. Harvest indicators visualization.

5. Discussion and conclusions: further research and model development

The strawberry growth model presented in this article has proven useful in programming predictive harvesting algorithms for robotic strawberry picking in a large strawberry plantation in Central Europe. The model provides data on the next-day distribution of ripe strawberries, which optimally schedules the fruit picking robots. The best harvesting efficiency can be achieved when the model is integrated with anticipatory robot coordination algorithms (Skulimowski, 2016) and AIoT systems in the greenhouse, providing real-time access to visual monitoring and other sensor data (Chen et al., 2020).

In addition to defining the states of the vegetation cycle from the perspective of strawberry fruit maturity, further information about each variety may be valuable during harvesting, including:

1. Past observations of the actual vegetation cycles from previous years under various climatic conditions in the vicinity of the modeled plantation.
2. A system of gathering and recording practical observations from robots and their supervisors.
3. Information on the use of phytohormones and on the effects of natural phytohormones (e.g. ethylene) on fruit ripening (An et al., 2022 ; Jo et al. 2022; Symons et al., 2012).
4. Characteristics of the influence of sunlight, temperature and humidity on the vegetation cycle of strawberry.

Additional information and observations that can increase model accuracy should be gradually incorporated based on crop observations during the strawberry vegetation season. We propose a hybrid reinforcement – supervised learning approach, where the reinforcement part uses the results of fruit scanning to update the model based on rewards derived from the actual and calculated fruit distribution. The supervised procedure is necessary to complement learning in cases where rotten or infected fruits cannot be identified by current robotic sensors. Various deep learning techniques dedicated to smart agriculture (Chaudhary et al., 2021) can be employed to enhance real-time the model learning.

Finally, the current Markov chain model can be replaced by random-fuzzy Markov chain (RFMC) models based on random-fuzzy state ranking. This class of methods, which can also be applied with fuzzy transition probabilities is particularly promising for deployment in highly autonomous robotized crops (Zhou et al., 2022). Another model extension can be obtained when discrete-time-dependent probabilities are considered as samples of a continuous process.

6. References

- Abd-Elrahman, A., Wu, F., Agehara, S., & Britt, K. (2021). Improving Strawberry Yield Prediction by Integrating Ground-Based Canopy Images in Modeling Approaches. *ISPRS Int. J. Geo-Inf.*, 10, art. #239. <https://doi.org/10.3390/ijgi10040239>.
- An, Q., Wang, K., Li, Z., Song, C., Tang X., & Song, J. (2022). Real-Time Monitoring Method of Strawberry Fruit Growth State Based on YOLO Improved Model, *IEEE Access*, 10, 124363-124372, doi: 10.1109/ACCESS.2022.3220234.
- Chaudhary, M., Gastli, M. S., Nassar, L., & Karray, F. (2021). Transfer Learning Application for Berries Yield Forecasting using Deep Learning. *Proceedings of the International Joint Conference on Neural Networks (IJCNN)*, 2021-July, pp. 1-8. doi: 10.1109/IJCNN52387.2021.9533530.
- Chen, S., Lin, J., Xu, A., Zhu, H., & Wu, W. (2020). Intelligent Strawberry Field Management and Control System. *2020 International Conference on Robots & Intelligent System (ICRIS)*, Sanya, China, pp. 21-23. doi: 10.1109/ICRIS52159.2020.00013.
- Clause, F. J., Mayorano, A. J., & Rubiales, V. A. (2007). Herrero Markovian Model Of Fruit Growth. *Applied Engineering in Agriculture*, 23(1), 105-110.
- Diel, M. I., Lúcio, A. D., Schmidt, D., de Lima Tartaglia, F., Tischler, A. L., & Lambrecht, D. M. (2022). Using nonlinear models to define production, production rate, and precocity of strawberry cultivars. *Revista Ceres*, 69(1), 55-61. doi: 10.1590/0034-737X202269010008.
- Fan, D., Wang, W., Hao, Q., & Jia, W. (2022). Do Non-climacteric Fruits Share a Common Ripening Mechanism of Hormonal Regulation? *Front. Plant Sci.*, 13, 923484. doi: 10.3389/fpls.2022.923484.
- Gao, Z., Shao, Y., Xuan, G., Wang, Y., Liu, Y., & Han, X. (2020). Real-time hyperspectral imaging for the in-field estimation of strawberry ripeness with deep learning. *Artificial Intelligence in Agriculture*, 4, 31–38, doi: 10.1016/j.aiia.2020.04.003.
- Ge, Y., Xiong, Y., & From, P. J. (2020). Classification of pickable and unpickable strawberries under farm conditions. *IEEE 16th International Conference on Automation Science and Engineering (CASE)*, Hong Kong, China, 2020, pp. 961-966. doi: 10.1109/CASE48305.2020.9217022.
- Jo, J. S., Kim, D. S., Jo, W. J., Sim, H. S., Lee, H. J., Moon, Y. H., Woo, U. J., Jung, S. B., Kim, S., Mo, X., Ahn, S. R., & Kim, S. K. (2022). Prediction of strawberry fruit yield based on cultivar-specific growth models in the tunnel-type greenhouse. *Horticulture Environment and Biotechnology*, 63(4), 467-476. doi: 10.1007/s13580-021-00416-0.
- Korsah, G. A., Stentz, A., & Dias, M. B. (2013). A comprehensive taxonomy for multi-robot task allocation. *International Journal of Robotic Research*, 32(12), 1495–1512. doi: 10.1177/0278364913496484.
- Lee, M. A., Monteiro, A., Barclay, A., Marcar, J., Miteva-Neagu, M., & Parker J. (2020). A framework for predicting soft-fruit yields and phenology using embedded, networked microsensors, coupled weather models and machine-learning techniques, *Computers and Electronics in Agriculture*, 168, art. #105103. doi: 10.1016/j.compag.2019.105103.
- Orchard, M., Muñoz-Poblete, C., Huirican, J. I., Galeas, P., & Rozas, H. (2019). Harvest Stage Recognition and Potential Fruit Damage Indicator for Berries Based on Hidden Markov Models and the Viterbi Algorithm. *Sensors*, 19, art. #4421, p.16. doi: 10.3390/s19204421.
- Ridho, M. F., & Irwan (2021). Strawberry Fruit Quality Assessment for Harvesting Robot using SSD Convolutional Neural Network. *8th International Conference on Electrical Engineering, Computer Science and Informatics (EECSI)*, 20-21 October 2021, pp. 157-162. doi: 10.23919/EECSI53397.2021.9624311.
- Sim, H. S., Kim, D. S., Ahn, M. G., Ahn, S. R., & Kim, S. K. (2020). Prediction of strawberry growth and fruit yield based on environmental and growth data in a greenhouse for soil cultivation with applied autonomous facilities. *Horticultural Science and Technology*, 38(6), 840-849. doi: 10.7235/HORT.20200076.
- Skulimowski, A. M. J. (2016). Anticipatory Control of Vehicle Swarms with Virtual Supervision. *Internet of Vehicles – Technologies and Services: 3rd International Conference, IOV 2016: Nadi, Fiji, Dec. 2016. Lecture Notes in Computer Science*, 10036, Springer, pp. 65–81, doi: 10.1007/978-3-319-51969-2_6.
- Skulimowski, A. M. J, & Karimi, M. (2023). Intelligent anticipatory mobile robot networks for autonomous fruit harvesting. In: *PP-RAI 4*, Lodz University of Technology Monographs No. 2437, Łódź, pp. 411–419. doi: 10.34658/9788366741928.65.
- Sønsteby, A, Solhaug, K. A., & Heide, O. M. (2016). Functional growth analysis of ‘Sonata’ strawberry plants grown under controlled temperature and day-length conditions. *Scientia Horticulturae*, 211, 36-33. doi: 10.1016/j.scienta.2016.08.003.
- Symons G.M., Chua Y.-J., Ross J. J., Quittenden L. J., Davies N. W., & Reid J. B. (2012). Hormonal changes during non-climacteric ripening in strawberry, *Journal of Experimental Botany*, 63(13), 4741–4750. doi: 10.1093/jxb/ers147.
- Tang, Y., Ma, X., Li, M., & Wang Y.-F. (2020). The effect of temperature and light on strawberry production in a solar greenhouse, *Solar Energy*, 195, 318-328. doi: 10.1016/j.solener.2019.11.070
- Twitchen, C., Else, M. A., & Hadley, P. (2021). The effect of temperature and light intensity on rate of strawberry fruit ripening. *Acta Horticulturae*, 1309, 643-648. doi: 10.17660/ActaHortic.2021.1309.92.
- Wendel, A., Underwood, J., & Walsh, K. (2018). Maturity estimation of mangoes using hyperspectral imaging from a ground based mobile platform, *Computers and Electronics in Agriculture*, 155, 298-313. doi: 10.1016/j.compag.2018.10.021.
- Zhou, H., Wang, X., Au, W.; Kang, H.-W., & Chen, C. (2022). Intelligent robots for fruit harvesting: recent developments and future challenges. *Precision Agriculture*, 23, 1856–1907. doi: 10.1007/s11119-022-09913-3.